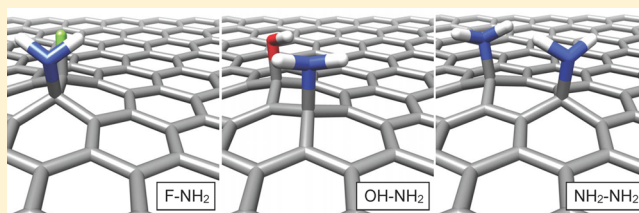


# Adsorption of NH<sub>2</sub> on Graphene in the Presence of Defects and Adsorbates

Chad E. Junkermeier, Dmitry Solenov, and Thomas L. Reinecke\*

Naval Research Laboratory, Washington, DC 20375, United States

**ABSTRACT:** Amine, NH<sub>2</sub>, is of interest as a linker between organic molecules and graphene in novel biotechnologies. We used ab initio electronic structure calculations to study NH<sub>2</sub> adsorption on graphene in the presence of surface defects and other adsorbates, including N, B, F, H, and OH. Amine is found to form a semi-ionic bond of 0.778 eV on pristine graphene. Its binding is found to be modified near other defects, and the adsorption energy is dependent on the neighbor order.



## INTRODUCTION

In recent years graphene has become one of the most interesting materials in nanotechnology in part because it opens opportunities in a range of technologies, including sensors, electronics, and hydrogen storage. However, some of the properties of graphene must be modified for it to be useful in these applications. Surface chemical functionalization is particularly effective at changing the properties of graphene because it is entirely made of surface atoms. A wide range of surface chemistries are being investigated to chemically functionalize graphene and to alter its properties.<sup>1–4</sup>

One class of functionalizations involve amines, the simplest being NH<sub>2</sub>. Amines are of interest because they are used in catalytic asymmetric synthesis,<sup>5</sup> chromatography,<sup>6</sup> and as a biconjugate linker<sup>7</sup> (i.e., between graphene and DNA). Previous calculations have shown that NH<sub>2</sub> binds at the on-top sites of pristine graphene with binding energies and mobilities that would allow it to diffuse readily across the surface.<sup>8</sup> It is known that adsorbates and surface defects can modify molecular adsorption properties.<sup>9,10</sup> Previous experimental<sup>11</sup> and theoretical work<sup>12</sup> on carbon nanotubes and graphene have shown that molecular adsorption energies often are increased at defects such as those related to oxygen and that these defects can modify sensor behaviors.<sup>13–15</sup>

Here we consider NH<sub>2</sub> adsorption on graphene in the presence of boron or nitrogen substitutional defects as well as fluorine, hydrogen, hydroxyl, or other amine adsorbates. We chose to look at these defects because depending on the growth processes involved<sup>16</sup> they can appear in amine–graphene systems. We discuss the computational methods used, the effects of a single defect, and then how neighboring defects affect the adsorption properties of NH<sub>2</sub> on graphene.

## METHODS

To find the ground-state structures of these graphene systems, we used Quantum Espresso<sup>17,18</sup> to do spin-unrestricted plane-wave density functional theory (DFT) calculations. We used

the Perdew–Burke–Ernzerhof (PBE) exchange–correlation parametrization of the generalized gradient approximation (GGA) with Vanderbilt ultrasoft pseudopotentials. To include weak dispersive interactions (van der Waals forces), semi-empirical dispersion terms (DFT-D) were included.<sup>19–21</sup> 12-by-12 rectangular graphene supercells and an interlayer spacing of 15 Å were used.

Figure 1a gives the relative positions of two graphene defects in our models. The primary defect is placed near the middle of the graphene sheet at position 0. The primary defect may be a substitutional B or N or an adsorbate: F, H, OH, or NH<sub>2</sub>. A second defect, always NH<sub>2</sub>, is adsorbed near the primary defect at one of the sites labeled 1–5. The positions labeled 1, 2, and 3 are, respectively, known as the ortho, para, and meta positions. In this work, when both defects are adsorbates they are both on the same side of the graphene sheet.

## RESULTS AND DISCUSSION

**Primary Defects.** We first consider NH<sub>2</sub> as a primary defect adsorbed alone on pristine graphene. We find that it adsorbs at an on-top site, as shown in Figure 1b. This results in the N atom being directly over the C atom, to which it is bound with a C–N–H angle of 107.8° and with each H atom pointing toward the center of neighboring benzyl rings. This arrangement of atoms is consistent with the polar nature of the amine molecule; the lone pair electrons of the N atom are oriented away from one of the neighboring p<sub>z</sub> orbitals. In this configuration, the C–N bond length is 1.518 Å, whereas the C atom to which the NH<sub>2</sub> molecule is attached is 0.583 Å out of the graphene plane. The C–N bond length indicates that the bond is semi-ionic. We find that the NH<sub>2</sub> has an adsorption energy of 0.778 eV, consistent with results given by Milowska et al.<sup>22</sup> The reason for the small adsorption energy is that NH<sub>2</sub>

Received: September 21, 2012

Revised: January 22, 2013

Published: February 5, 2013



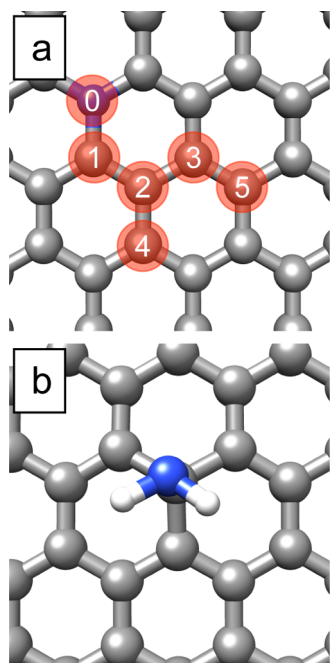


**Figure 1.** (a) Section of the rectangular graphene supercell where the numbers on the atoms represent the neighbor order with respect to the primary defect position 0 in the graphene lattice. In this example, the primary defect is a substitutional N atom. The atoms labeled 1, 2, and 3 are, respectively, in the ortho, meta, and para positions in relation to position 0. (b) An amine group is shown on the graphene surface where the blue atom is a N atom and the white atoms are H atoms.

has an electron that it would like to donate, whereas the carbon atoms in graphene already have full shells.

To understand the nature of the bond between graphene and  $\text{NH}_2$ , we examined their electronic density of states (DOS). Figure 2a gives the DOS of defect-free graphene and the projected density of states (PDOS) of isolated  $\text{NH}_2$ . Comparing the relative energies of the highest occupied molecular orbital (HOMO) and lowest unoccupied molecular orbital (LUMO) states of  $\text{NH}_2$  with the Fermi energy of

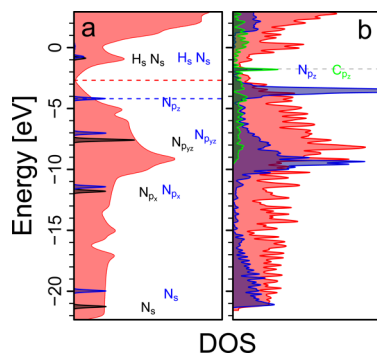


**Figure 2.** Density of states of graphene– $\text{NH}_2$  systems. (a) Spin-polarized DOS of isolated graphene (red) and isolated  $\text{NH}_2$  (black and blue (electron spin up and spin down, respectively)) at infinite separation. The black and blue labels situated to the right of the peaks indicate which atomic orbital(s) contribute most to a particular  $\text{NH}_2$  molecular orbital. (b) DOS of the graphene sheet with one  $\text{NH}_2$  molecule adsorbed on it is shown in red. PDOS of the  $p_z$  orbital of the  $\text{NH}_2$  N atom is blue. PDOS of the  $p_z$  orbital of the C atom to which the N atom is bonded is green.

graphene, we can determine if in the combined system charge should be transferred via band alignment.<sup>23</sup> If the HOMO level of  $\text{NH}_2$  is above the Fermi energy of graphene, then charge transfers from  $\text{NH}_2$  into the graphene conduction band. If the  $\text{NH}_2$  LUMO is below the graphene Fermi energy, then charge transfers from the graphene valence band into the  $\text{NH}_2$  LUMO states. Our results show that the HOMO of isolated  $\text{NH}_2$  is  $\sim 2$  eV below the Fermi energy of graphene, whereas the  $\text{NH}_2$  LUMO is several electronvolts above the Fermi energy. Thus, in the  $\text{NH}_2$ –graphene system any charge transfer is not due to band alignment. We find that the  $\text{NH}_2$  HOMO is located on the  $N_{p_z}$  orbital, in an energy region where the carbon  $p_z$  orbitals (in the form of  $\pi$ -bonds) dominate. This suggests that a covalent C–N bond may be formed between graphene and  $\text{NH}_2$ . Figure 2b shows the effect that the bonding has on the PDOS. When the  $\text{NH}_2$  molecule is adsorbed on graphene a defect peak appears at the Fermi level, disrupting the Dirac point. The PDOS shows that it is due to a change in the  $p_z$  orbital of the C atom to which the adsorbate is bound with a corresponding peak from the  $N_{p_z}$  orbital. Thus, whereas  $\text{NH}_2$  would rather donate an electron and the C atoms have full shells via the  $\sigma$  and  $\pi$  bonds, a C atom and an  $\text{NH}_2$  molecule can form a weak bond between the  $N_{p_z}$  and  $C_{p_z}$ . These features are consistent with the C–N bond being semi-ionic.

We now consider the other primary defects of interest here. Table 1 gives the binding energies of each primary defect, the

**Table 1.** Adsorption Energy, Charge Transfer, and Adsorbate Bond Length for the Primary Defects<sup>a</sup>

defect	energy [eV]	adsorbate charge [e]	C charge [e]	bond length [Å]
B	5.799	0.115	NA	NA
N	7.017	0.011	NA	NA
F	2.310	−0.394	0.228	1.678
H	1.324	0.224	−0.158	1.110
$\text{NH}_2$	0.778	0.030	0.108	1.518
OH	1.227	−0.136	−0.187	1.407

<sup>a</sup>Positive adsorbate charge value means electrons have been donated by the atom (molecule), leaving a positively charged entity. B and N are substitutional defects in the graphene lattice and thus do not have C atom charge difference or bond lengths from C. The bond lengths reported for  $\text{NH}_2$  and OH are the C–N and C–O distances, respectively.

Löwdin charge transfer into or out of the defect, and the C–X, where X = {F, H, O (in OH), N (in  $\text{NH}_2$ )}, the bond length between an adsorbate and the C atom it is attached to. For a substitutional defect the formation energies in Table 1 were computed by

$$\Delta E = (E_{\text{GRY}} + E_{\text{C}}) - (E_{\text{GR}} + E_{\text{Y}}) \quad (1)$$

where  $E_{\text{GR}}$  is the energy of the graphene supercell,  $E_{\text{Y}}$  is the energy of a lone N (or B) atom,  $E_{\text{GRY}}$  is the energy of the graphene supercell with the N (or B) atom replacing one of the C atoms, and  $E_{\text{C}}$  is the energy of a lone C atom. A negative  $\Delta E$  indicates an exothermic process. In cases when the primary defect is an adsorbate, the energy was computed using

$$\Delta E = E_{\text{GRZ}} - (E_{\text{GR}} + E_{\text{Z}}) \quad (2)$$

where  $E_{\text{GRZ}}$  is the energy of the combined graphene and adsorbate system and  $E_{\text{Z}}$  is the energy of the adsorbate. Among the adsorbates studied here, F has the largest adsorption energy

when adsorbed alone and  $\text{NH}_2$  has the smallest. The B and N substitutional defects are found to be exothermic, consistent with expectations.<sup>24</sup> Comparing the C–X bond lengths of the primary adsorbate defects with the accepted covalent bond lengths,<sup>25</sup> we find that all of them are consistent with the bonding being semi-ionic.

In Figure 3, we illustrate the effect that adsorbate defects have on the calculated charge of the C atoms in the graphene

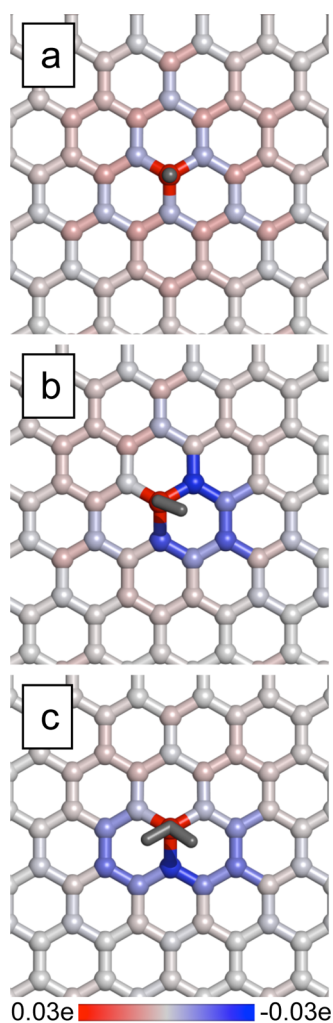


**Figure 3.** Effect of adsorbates on the charge in surrounding C atoms. The neutral value is set to the (Löwdin) charge on the C atoms in clean graphene, and differences from that value are colored in shades of red or blue. The dark-gray atoms show the position of adsorbates. The color of the C atom to which the adsorbate is attached is not indicative of the charge difference on that atom; when F is attached, the C atom has a charge difference of 0.23 e, when  $\text{NH}_2$  is adsorbed, the charge difference on the C atom is 0.11 e; all other C atoms are represented by the color on the atom. (a) F adsorption, (b) OH adsorption, and (c)  $\text{NH}_2$  adsorption.

sheet. There the colors of the C atoms represent the change in the charge. Charge transfer is due to the difference in electronegativities, which gives a charge transfer between the C atom and the adsorbate. In Figure 3a for F adsorption, we see that more than just the C atom bonded to the F atom is involved; while most of charge difference is in that C atom, the nearby C atoms also show small charge transfers. The charge transfer on the neighboring C atoms is an order of magnitude

smaller than that on the C to which the F is bound. From columns 3 and 4 of Table 1, we see that the charge removed from C atom is less than the charge transferred to the F atom, and thus charge must be pulled from other nearby carbon atoms.

The charge transfer and polarization in Figure 3 may influence clustering of multiple adsorbates and contribute to other effects, such as distortion of the lattice.<sup>26</sup> Figure 3a shows a triangular symmetry of the charge distribution within the graphene sheet around the F adatom. Triangular symmetry has been related to the low energy of clustering of H on a graphene sheet by Casolo et al.<sup>27</sup> It is likely that the lack of triangular symmetry seen in Figure 3b,c for OH and  $\text{NH}_2$  adsorption suggests that these molecules may exhibit different high concentration adsorption conformations than those for H and F.

**Secondary Defects.** Figure 4 gives the adsorption energies of a secondary  $\text{NH}_2$  in the presence of other (primary)

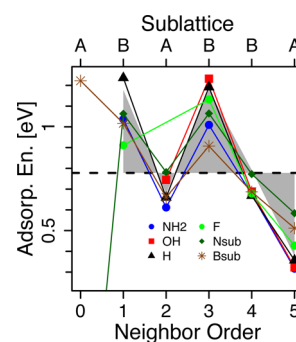


**Figure 4.** Adsorption energies of the secondary  $\text{NH}_2$  as a function of neighbor order from the primary defects listed in the Figure. The dashed line represents the adsorption energy  $\text{NH}_2$  molecule. The gray region shows an analytical description based on the nearest-neighbor tight binding model of graphene, as described in the text. The axis labeled “Sublattice” indicates the sublattice (A or B) of the C atom to which the secondary defect is attached.

defects.<sup>28</sup> The energies are given by eq 2, where  $E_{\text{GR}}$  now represents the energy of the combined graphene and primary defect system and  $E_{\text{GR}_Z}$  is the energy of the combined graphene, primary defect, and  $\text{NH}_2$  system. Thus, the total energy of the primary defect adsorbed on graphene is used as the zero of the energy when a secondary  $\text{NH}_2$  molecule is adsorbed. The secondary  $\text{NH}_2$  adsorption energies have similar dependencies on separation from the several primary defects. The separation dependence is shaped primarily by the electronic structure of graphene’s conjugated  $\pi$  electrons, as we discuss below. The relative energies when both adsorbates are on the same side of the graphene sheet are similar to the trend that Casolo et al. give in table 2 of ref 27 for two H atoms adsorbed on the same side of the sheet.

Substitutional nitrogen defects may occur whenever amines are adsorbed onto graphene.  $\text{NH}_2$  does not form a stable bond directly with the substitutional N. This is due to both N atoms in the bond wanting to donate an electron. The adsorption energy of the  $\text{NH}_2$  on a first- or third-order neighbor site of the substitutional N is nearly 37% larger than the adsorption energy of a singly adsorbed  $\text{NH}_2$ . The adsorption energy of the secondary  $\text{NH}_2$  when it is on the second- or third-order neighbor sites is closer to the singly adsorbed  $\text{NH}_2$  energy. The secondary adsorption energy of an  $\text{NH}_2$  in the presence of

another NH<sub>2</sub> is consistently lower than when NH<sub>2</sub> adsorbs near a substitutional N. This suggests that in experiment we should expect to see more NH<sub>2</sub> adsorbed onto the graphene when substitutional N are present than when only NH<sub>2</sub> adsorbates are present.

To understand the variation of adsorption energy of secondary NH<sub>2</sub> with distance, we recall that the primitive cell of graphene contains two carbon atoms and forms a bipartite lattice.<sup>29,30</sup> Lattice sites related to these two different atoms of the primitive cell by symmetry operations form two sublattices, A and B. From DFT results in Figure 4, we notice that adsorption energy changes depending on whether the defects are on the same sublattice, for example, both on A sublattice sites, or are on different sublattices. The DFT calculations include electron orbitals in a wide range of energies including many effects, for example, elastic deformation of the lattice. However, only orbitals in a narrow range of energies near the chemical potential that form the conduction network (conjugated  $\pi$  electrons) are substantially affected<sup>30</sup> by the bipartite nature of the lattice. This suggests that conduction electrons play the dominant role in defining the variation of adsorption energy with distance between the two defects.

To demonstrate this, we model the conjugated  $\pi$  electrons by a tight-binding Hamiltonian, in which electrons from carbon  $p_z$  orbitals hop between neighboring  $p_z$  orbitals of carbon with amplitude  $t$ .<sup>29</sup> Adsorbates disrupt this hopping by altering local electronic configurations, thus introducing scattering centers. The simplest distance-dependent contribution to the adsorption energy of a pair of adsorbates involves two such scattering events (vertices) and is given by a polarization bubble  $\Pi(\mathbf{R})$ , where  $\mathbf{R}$  is the distance between the two vertices. Because of bipartite nature<sup>30</sup> of the graphene's lattice,  $\Pi(\mathbf{R})$  depends on the sublattice index

$$\Pi_{ij}(\mathbf{R}) = \int \frac{d\omega d\mathbf{q} d\mathbf{q}'}{(2\pi)^5} e^{i\mathbf{R}(\mathbf{q}-\mathbf{q}')} G_{ij}(i\omega, \mathbf{q}) G_{ji}(i\omega, \mathbf{q}') \quad (3)$$

where  $i$  and  $j$  refer to A or B sublattices.<sup>29</sup> Near the half-filling, the spectrum of graphene has two nonequivalent conical valleys  $\mathbf{K}$  and  $\mathbf{K}'$ .<sup>30</sup> The characteristic momentum difference  $\mathbf{K} - \mathbf{K}'$  between the two adjacent valleys gives rise to fast spatial oscillations. The momentum integration in eq 3 runs over the entire Brillouin zone; however, at (or near) the half-filling the dominant contributions come from the regions near the conical points  $\mathbf{K}(\mathbf{K}')$ . The lattice Green's functions on different sublattices  $G_{AB}(i\omega, \mathbf{K} + \mathbf{q})$  and  $G_{AB}(i\omega, \mathbf{K}' + \mathbf{q})$  acquire an additional phase factors of  $(q_x + iq_y)/q$  and  $(q_x - iq_y)/q$ , respectively, when  $|\mathbf{q}| \ll |\mathbf{K}|$ .<sup>29,31</sup> This sublattice-dependent phase factors together with  $e^{i\mathbf{R}(\mathbf{q}-\mathbf{q}')}$  produce an overall oscillatory factor. In particular, when the adsorbates are on the same sublattice

$$e^{i\mathbf{R}(\mathbf{q}-\mathbf{q}')} \rightarrow |e^{i\mathbf{R}\mathbf{K}} + e^{i\mathbf{R}\mathbf{K}'}|^2 = 2 + 2 \cos \mathbf{R}(\mathbf{K} - \mathbf{K}') \quad (4)$$

whereas when the adsorbates are on the different sublattices

$$\begin{aligned} e^{i\mathbf{R}(\mathbf{q}-\mathbf{q}')} \frac{q_x \pm iq_y}{q} &\rightarrow |e^{i\theta+i\pi/2} e^{i\mathbf{R}\mathbf{K}} + e^{-i\theta-i\pi/2} e^{i\mathbf{R}\mathbf{K}'}|^2 \\ &= 2 + 2 \cos\{\mathbf{R}(\mathbf{K} - \mathbf{K}') + 2\theta + \pi\} \end{aligned} \quad (5)$$

where  $\theta$  is the angle between  $\mathbf{R}$  and  $\mathbf{K}' - \mathbf{K}$ . In addition, the particle-hole symmetry of the Hamiltonian at half-filling requires  $\Pi_{AA}$  and  $\Pi_{AB}$  to have opposite signs, as discussed in detail by Saremi.<sup>31</sup> The magnitude of eq 3 depends on details,

such as strength of the scattering, polarization of the bonds, and chemical potential, and is cumbersome to evaluate. However, the above symmetry relation together with eqs 4 and 5 provides a qualitative description of the oscillatory behavior found with DFT calculations. In Figure 4, the overall magnitude of the analytical result is adjusted to match the DFT data. Effects due to lower-laying orbitals, such as, for example, local strain in graphene lattice, is likely to play a role in deviation of the adsorption energies from the energy given by the above qualitative description. This can be especially pronounced at short distances, where local deformation of C–C bonds can play an important role.<sup>26</sup>

The C–X, where X = {F, H, O (in OH), N (in NH<sub>2</sub>)}, bond lengths for primary defects and the secondary NH<sub>2</sub> for different distances between defect sites are shown in Figure 5. In Figure

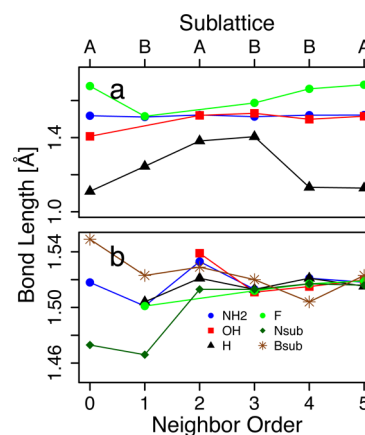


**Figure 5.** Bond lengths: (a) The bond length between the primary adsorbate (C– bond) and carbon atom to which it is bound. This excludes the substitutional defects. (b) The bond length between carbon and the N atom in the secondary NH<sub>2</sub> (C–N bond). NH<sub>2</sub> can be both a primary and secondary defect. The Nsub and Bsub designations are for the substitutional N and B atoms and thus do not have values in panel a.

5a, we give the values for the bond lengths for the primary defects adsorbed on top of a carbon atom. The bond lengths for the secondary NH<sub>2</sub> (for the bond between nitrogen and carbon) are given in Figure 5b. The variation in the C–N bond length for the secondary NH<sub>2</sub> defect placed at different positions relative to the primary defect (the first through the fifth order neighbor sites) is <5%. The C–X bond changes as much as 25% with distance from the NH<sub>2</sub> molecule. This variation, together with the variation in charge transfer discussed below affects the scattering of conduction electrons on primary and secondary defects and thus can contribute to the variation of the adsorption energies of the secondary NH<sub>2</sub>.

Figure 6a,b show the total (Löwdin) charge transferred into the primary and secondary defects, respectively, when two defects are present. The charge transferred into the primary defect, of any particular type should be compared with the single defect value listed in Table 1 for the same type of defect. Similarly, the charge transferred into the secondary defect, always an NH<sub>2</sub> molecule, should be compared with the single NH<sub>2</sub> value listed in Table 1 for NH<sub>2</sub>. The values shown in Figure 6 have large deviations from the single defect cases. The average deviation of the charge transfer is about 44 and 80% for the primary and secondary defects, respectively. The largest deviations are observed in the cases where the secondary NH<sub>2</sub>

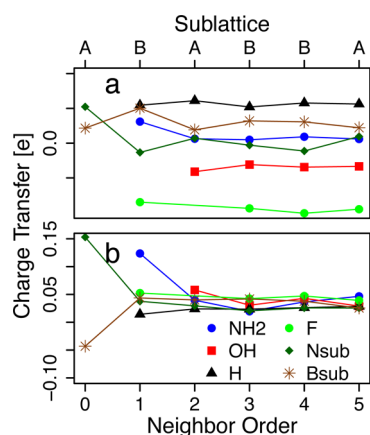


**Figure 6.** Löwdin charge transfer into each defect when NH<sub>2</sub> is adsorbed near a primary defect. (a) Charge transfer into the primary defect. (b) Charge transfer into the NH<sub>2</sub> defect. A positive value means electrons have been donated by the atom (molecule), leaving a positively charged entity.

is adsorbed on a substitutional defect. In these cases the deviation can be attributed to the fact that NH<sub>2</sub> forms a direct bond with substitutional defect instead of a carbon. There is also large deviation in the charge transferred when NH<sub>2</sub> is located near (first or second neighbor) an OH or NH<sub>2</sub>. In the case of two adsorbed NH<sub>2</sub> groups, or a NH<sub>2</sub> and OH pairing, the large deviation in charge transfer is likely partially due to inaccuracies in computing the Löwdin charge. In these cases, the adsorbed molecules are rotated around their C-X bonds in such a way as to indicate hydrogen bonding. Hydrogen bonding can affect the polarization of the adsorbate group, thus changing the distribution of charge within the group. In this case the Löwdin calculation does not attribute some of the charge to the atoms, where it is expected to reside. Overall, we find that the difference in charge transfer for the cases of a pair of defects and a lone defect decreases as neighbor order increases and defects become more isolated from each other.

## SUMMARY

In summary, we studied the bonding of NH<sub>2</sub> molecules near other graphene defects. These defects include adatoms, ad molecules, and substitutional defects. The binding energy of an NH<sub>2</sub> depends on its distance from a primary defect. The distance dependence is due to scattering processes in graphene's conjugated  $\pi$  electrons. At a particular distance from the primary defect the adsorption energy of NH<sub>2</sub> also depends on the type of primary defect. We find that NH<sub>2</sub> chemisorbs to the graphene surface with a semi-ionic bond.

## AUTHOR INFORMATION

### Corresponding Author

\*E-mail: reinecke@nrl.navy.mil.

### Notes

The authors declare no competing financial interest.

## ACKNOWLEDGMENTS

This work was partially supported by the U.S. Office of Naval Research. The DoD High Performance Computing Modernization Program provided computer resources. C.E.J. and D.S. are National Research Council Postdoctoral Associates.

## REFERENCES

- (1) Robinson, J. T.; Burgess, J. S.; Junkermeier, C. E.; Badescu, S. C.; Reinecke, T. L.; Perkins, F. K.; Zalalutdinov, M. K.; Baldwin, J. W.; Culbertson, J. C.; Sheehan, P. E.; Snow, E. S. Properties of Fluorinated Graphene Films. *Nano Lett.* **2010**, *10*, 3001–3005.
- (2) Wheeler, V.; Garces, N.; Nyakiti, L.; Myers-Ward, R.; Jernigan, G.; Culbertson, J.; Eddy, C., Jr.; Gaskill, D. K. Fluorine Functionalization of Epitaxial Graphene for Uniform Deposition of Thin High-K Dielectrics. *Carbon* **2012**, *50*, 2307–2314.
- (3) Wang, M.; Huang, W.; Chan-Park, M. B.; Li, C. M. Magnetism in Oxidized Graphenes with Hydroxyl Groups. *Nanotechnology* **2011**, *22*, 105702.
- (4) Åkesson, J.; Sundborg, O.; Wahlström, O.; Schröder, E. A van der Waals Density Functional Study of Chloroform and Bromoform on Graphene. *arXiv* **2012**, arXiv:1206.1972v1 [cond-mat.mtrl-sci].
- (5) Notz, W.; Tanaka, F.; Barbas, C. F. Enamine-Based Organocatalysis with Proline and Diamines: The Development of Direct Catalytic Asymmetric Aldol, Mannich, Michael, and Diels-Alder Reactions. *Acc. Chem. Res.* **2004**, *37*, 580–591 (PMID: 15311957).
- (6) Kraml, C. M.; Zhou, D.; Byrne, N.; McConnell, O. Enhanced Chromatographic Resolution of Amine Enantiomers As Carbobenzyloxy Derivatives in High-Performance Liquid Chromatography and Supercritical Fluid Chromatography. *J. Chromatogr., A* **2005**, *1100*, 108–115.
- (7) Wang, J.-g.; Prodan, E.; Car, R.; Selloni, A. Band Alignment in Molecular Devices: Influence of Anchoring Group and Metal Work Function. *Phys. Rev. B* **2008**, *77*, 245443.
- (8) Erni, R.; Rossell, M. D.; Nguyen, M.-T.; Blankenburg, S.; Passerone, D.; Hartel, P.; Alem, N.; Erickson, K.; Gannett, W.; Zettl, A. Stability and Dynamics of Small Molecules Trapped on Graphene. *Phys. Rev. B* **2010**, *82*, 165443.
- (9) Hornekær, L.; Rauls, E.; Xu, W.; Šljivančanin, i. c. v.; Otero, R.; Stensgaard, I.; Lægsgaard, E.; Hammer, B.; Besenbacher, F. Clustering of Chemisorbed H(D) Atoms on the Graphite (0001) Surface due to Preferential Sticking. *Phys. Rev. Lett.* **2006**, *97*, 186102.
- (10) Lin, Y.; Ding, F.; Yakobson, B. I. Hydrogen Storage by Spillover on Graphene As a Phase Nucleation Process. *Phys. Rev. B* **2008**, *78*, 041402.
- (11) Robinson, J. A.; Snow, E. S.; Badescu, S. C.; Reinecke, T. L.; Perkins, F. K. Role of Defects in Single-Walled Carbon Nanotube Chemical Sensors. *Nano Lett.* **2006**, *6*, 1747–1751.
- (12) Woods, L. M.; Badescu, S. C.; Reinecke, T. L. Adsorption of Simple Benzene Derivatives on Carbon Nanotubes. *Phys. Rev. B* **2007**, *75*, 155415.
- (13) Snow, E. S.; Perkins, F. K.; Houser, E. J.; Badescu, S. C.; Reinecke, T. L. Chemical Detection with a Single-Walled Carbon Nanotube Capacitor. *Science* **2005**, *307*, 1942–1945.
- (14) Zalalutdinov, M. K.; Robinson, J. T.; Junkermeier, C. E.; Culbertson, J. C.; Reinecke, T. L.; Stine, R.; Sheehan, P. E.; Houston, B. H.; Snow, E. S. Engineering Graphene Mechanical Systems. *Nano Lett.* **2012**, *12*, 4212–4218.
- (15) Robinson, J. T.; Zalalutdinov, M. K.; Junkermeier, C. E.; Culbertson, J. C.; Reinecke, T. L.; Stine, R.; Sheehan, P. E.; Houston, B. H.; Snow, E. S. Structural Transformations in Chemically Modified Graphene. *Solid State Commun.* **2012**, *152*, 1990–1998.
- (16) Baraket, M.; Stine, R.; Lee, W. K.; Robinson, J. T.; Tamana, C. R.; Sheehan, P. E.; Walton, S. G. Aminated Graphene for DNA Attachment Produced via Plasma Functionalization. *Appl. Phys. Lett.* **2012**, *100*, 233123.
- (17) Giannozzi, P.; et al. QUANTUM ESPRESSO: a Modular and Open-Source Software Project for Quantum Simulations of Materials. *J. Phys.: Condens. Matter* **2009**, *21*, 395502.
- (18) All of the calculations were performed using Quantum Espresso version 4.2 on a SGI Altix ICE 8200 machine. We used the pseudopotentials C.pbe-van\_ak.UPF, F.pbe-n-van.UPF, H.pbe-van\_ak.UPF, N.pbe-van\_ak.UPF, and O.pbe-van\_ak.UPF from <http://www.quantum-espresso.org>. Much of the system setup and data analysis (that not specifically performed by Quantum Espresso) was created or

performed using Clojure.<sup>32</sup> Figures were produced using UCSF's Chimera<sup>33</sup> and R.<sup>34</sup>

(19) Grimme, S. Semiempirical GGA-Type Density Functional Constructed with a Long-Range Dispersion Correction. *J. Comput. Chem.* **2006**, *27*, 1787–1799.

(20) Barone, V.; Casarin, M.; Forrer, D.; Pavone, M.; Sambri, M.; Vittadini, A. Role and Effective Treatment of Dispersive Forces in Materials: Polyethylene and Graphite Crystals As Test Cases. *J. Comput. Chem.* **2009**, *30*, 934–939.

(21) Grimme, S. Density Functional Theory with London Dispersion Corrections. *Wiley Interdiscip. Rev.: Comput. Mol. Sci.* **2011**, *1*, 211–228.

(22) Milowska, K.; Birowska, M.; Majewski, J. A. Structural and Electronic Properties of Functionalized Graphene. *Acta Phys. Pol., A* **2011**, *120*, 842–844.

(23) Leenaerts, O.; Partoens, B.; Peeters, F. M. Adsorption of H<sub>2</sub>O, NH<sub>3</sub>, CO, NO<sub>2</sub>, and NO on Graphene: A First-Principles Study. *Phys. Rev. B* **2008**, *77*, 125416.

(24) Panchakarla, L. S.; Subrahmanyam, K. S.; Saha, S. K.; Govindaraj, A.; Krishnamurthy, H. R.; Waghmare, U. V.; Rao, C. N. R. Synthesis, Structure, and Properties of Boron- and Nitrogen-Doped Graphene. *Adv. Mater.* **2009**, *21*, 4726–4730.

(25) Lide, D. R. *CRC Handbook of Chemistry and Physics*, 92nd ed.; CRC Press/Taylor and Francis: Boca Raton, FL, 2011.

(26) Nguyen, M.-T.; Erni, R.; Passerone, D. Two-Dimensional Nucleation and Growth Mechanism Explaining Graphene Oxide Structures. *Phys. Rev. B* **2012**, *86*, 115406.

(27) Casolo, S.; Løvrik, O. M.; Martinazzo, R.; Tantardini, G. F. Understanding Adsorption of Hydrogen Atoms on Graphene. *J. Chem. Phys.* **2009**, *130*, 054704.

(28) There is not a data point given for the case of F as the primary defect and NH<sub>2</sub> in the meta position because during the relaxation calculation a H–F bond forms and then HF desorbs from graphene. There is also no data point for OH as the primary defect and NH<sub>2</sub> in the ortho position because NOH<sub>3</sub> is created and desorbed in that case.

(29) Castro Neto, A. H.; Guinea, F.; Peres, N. M. R.; Novoselov, K. S.; Geim, A. K. The Electronic Properties of Graphene. *Rev. Mod. Phys.* **2009**, *81*, 109–162.

(30) Semenoff, G. W. Condensed-Matter Simulation of a Three-Dimensional Anomaly. *Phys. Rev. Lett.* **1984**, *53*, 2449–2452.

(31) Saremi, S. RKKY in Half-Filled Bipartite Lattices: Graphene As an Example. *Phys. Rev. B* **2007**, *76*, 184430.

(32) Hickey, R. The Clojure Programming Language. In *DLS '08 Proceedings of the 2008 Symposium on Dynamic Languages*; ACM: New York, 2008. <http://doi.acm.org/10.1145/1408681.1408682>.

(33) Pettersen, E. F.; Goddard, T. D.; Huang, C. C.; Couch, G. S.; Greenblatt, D. M.; Meng, E. C.; Ferrin, T. E. UCSF Chimera—A Visualization System for Exploratory Research and Analysis. *J. Comput. Chem.* **2004**, *13*, 1605–1612.

(34) R Development Core Team. *R: A Language and Environment for Statistical Computing*; R Foundation for Statistical Computing: Vienna, Austria, 2011.